ISSN 1063-7826, Semiconductors, 2010, Vol. 44, No. 2, pp. 228–232. © Pleiades Publishing, Ltd., 2010.
Original Russian Text © L.B. Karlina, A.S. Vlasov, M.M. Kulagina, E.P. Rakova, N.Kh. Timoshina, V.M. Andreev, 2010, published in Fizika i Tekhnika Poluprovodnikov, 2010, Vol. 44, No. 2, pp. 240–245.

PHYSICS OF SEMICONDUCTOR DEVICES

Highly Efficient Photovoltaic Cells Based on $In_{0.53}Ga_{0.47}As$ Alloys with Isovalent Doping

L. B. Karlina^, A. S. Vlasov, M. M. Kulagina, E. P. Rakova, N. Kh. Timoshina, and V. M. Andreev

Ioffe Physical-Technical Institute, Russian Academy of Sciences, Polytekhnicheskaya ul. 26, St. Petersburg, 194021 Russia

^e-mail: karlin@mail.ioffe.ru

Submitted June 22, 2009; accepted for publication June 29, 2009

Abstract—The effect of isovalent doping with P on the surface and bulk properties of the $In_{0.53}Ga_{0.47}As$ alloy (below, InGaAs) was evaluated from variations in the photoluminescence and transmission spectra. It is established that isovalent doping decreases the nonradiative recombination rate in the bulk and on the surface of doped layers. The use of additional isovalent doping provided an improvement of parameters of the narrow-gap InGaAs-based solar cell used for the conversion of the concentrated solar radiation. The maximum efficiency of photovoltaic conversion in a spectral range of 900–1840 nm was 7.4–7.35% at a ratio of concentration of the solar radiation of 500–1000 for the AM1.5D Low AOD spectrum.

DOI: 10.1134/S1063782610020168

1. INTRODUCTION

The development of alternative energy sources requires developing environmentally safe and inexpensive methods of production of semiconductor devices for these purposes. The prospects of the further increase in efficiency of photovoltaic conversion of the solar energy are associated both with the use of monolithic concentrator elements and with maximally effective transformation of the split solar spectrum by separate photoconverters with different band gap. Devices based on narrow-gap InGaAs alloys are promising for conversion in the infrared region of the solar spectrum.

Currently, the solar cells based on the InP/InGaAs heterostructure are fabricated mainly by MOCVD [1, 2]. In [3–5], it is shown that it is possible to fabricate the highly efficient devices by liquid-phase epitaxy and subsequent diffusion of zinc into the grown layer to form the *p–n* junction. The developed method of simultaneous diffusion of isovalent impurity of P and Zn from a local source in a flow system provides high reproducibility of parameters of the diffusion layers. This is due to minimization of the number of production operations affecting this process. High efficiency is provided by the simplicity of the equipment used.

Conversion of solar energy at the concentration ratio in the range of 100–1000 makes additional demands on the used photoconverters, specifically, the possibility of operation of the cell at high current densities (1–20 A/cm^2) while retaining a high value of the fill factor of the current–voltage characteristic. This parameter of the solar cell is determined by the magnitude of the dark current of the photoconverter and by the possibility of formation of the low-resistance contacts. Before the beginning of diffusion of the doping impurity (Zn), the grown structure is in the reactor in hydrogen atmosphere at a constantly increasing temperature until a specified value is established (about 600°C). It is known that annealing in hydrogen leads to the competition of processes of defect formation and hydrogen passivation of defects in III–V materials [6]. The additional isovalent doping of the starting InGaAs layer with P before the start of the diffusion of the doping impurity can substantially affect the bulk and surface properties of the *n*- and *p*-layers of the alloy and device parameters.

This study is devoted to examination of the fabrication process of highly efficient narrow-gap cells based on the InGaAs/InP heterostructure. The results of study of preliminary diffusion of P on the material properties and devices obtained on its base are presented.

2. FABRICATION OF PHOTOCELLS AND EXPERIMENTAL PROCEDURE

As the main solar cell design, an inverted element was chosen [7] with a wide-gap window—the InP substrate (Fig. 1). In contrast with the conventional design, the invert structure of the photocell implies the formation of a comparatively thick base *p*-region of the cell by the diffusion. The *n*-InGaAs region adjoining the *n*-InP buffer layer is the emitter. The solar radiation is introduced through the InP substrate. Similarly to the invert cascade solar cells [8], this design of the narrow-gap cell possesses some advantages compared with the usual design, in which a thin heavily doped layer plays the role of emitter. In our case, the contact to the emitter is mounted on the

surface of the *n*-InP substrate. The formation of a thick diffusion layer considerably simplifies control over the diffusion process and decreases the sheet resistance of the base region. The InP buffer layer and the layer of the $In_{0.53}Ga_{0.47}As$ alloy 3–5 μm thick with an impurity concentration of $(1–5) \times 10^{17}$ cm^{-3} were grown on an InP substrate 300–400 μm thick and with a carrier concentration of $(0.6–1) \times 10^{18}$ cm^{-3} by liquid-phase epitaxy.

The subsequent diffusion of P or P and Zn was performed in a flow system in hydrogen atmosphere. The sources consisted of the drops of Sn–InP and Sn–InP–Zn placed into special cells over the sample at a temperature of 570–600°C. The structure was sequentially transported under the sources. The diffusion proceeded from the gas phase [3–5]. It should be noted that diffusion of only Zn (without P) was not carried out, since the advantage of simultaneous diffusion of Zn and P for obtainment of the *p*-InGaAs layers had been shown before [4]. In this case, the process of fabrication of *p–n* junctions in the alloys is one-stage and does not require forming protective masks on the surface of the semiconductor for additional local diffusion or for the growth of additional subcontact heavily doped layers. The face contacts on the surface of the *n*-InP substrate were formed by the deposition of the Au/Ge, Ni, Au composition with the subsequent firing. The back contact to the *p*-InGaAs base layer obtained by diffusion was formed via sequential deposition of Cr and Au. No additional firing was carried out. Enhancement of contacts was attained by electrolytic deposition of Au. The antireflection coating consisted of sequentially deposited ZnS/MgF_2 layers.

The effect of P on the surface and bulk properties of the InGaAs layers was evaluated from the variation in the photoluminescence and transmission spectra. The photoluminescence spectra were measured at $T = 77$ and 300 K in the wavelength range of 1300–1800 nm on an MDR-23 spectrometer with resolution no worse than 5 nm. For the excitation, the Nd :YAG laser with a wavelength of 532 nm and radiation intensity as high as 200 mW was used. The form of the photoluminescence (PL) spectra—the location of the peaks and half-width of the bands as well as the ratio of intensities—for all samples under study was analyzed under conditions of identical intensity of excitation. The excitation power density when studying the InGaAs layers was ~100 W/cm^2.

The concentration of free charge carriers was determined by the Raman scattering via the analysis of the effects of interaction of longitudinal optical vibrations with the plasma of free carriers [9]. The concentration of isovalent impurity (P) according to the measurements obtained by secondary ion mass spectroscopy in the InGaAs layers is 10^{20} cm^{-3}.

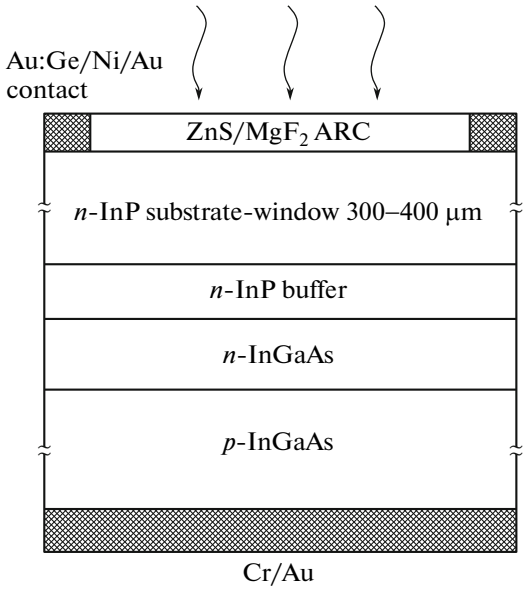

Fig. 1. Schematic structure of the InP/InGaAs-based invert solar cell. The InP substrate is irradiated.

3. EXPERIMENTAL RESULTS

3.1. n-InGaAs Layers

Figure 2 shows the PL spectra of the lattice-matched InGaAs alloys before and after diffusion of P. In the studied layers, the background concentration of free electrons was $(3–5) \times 10^{17}$ cm^{-3}. Diffusion of P was performed at a constant temperature of 600°C for 20 min.

It is evident from Fig. 2 that doping with P leads to an increase in the PL intensity. The ratio of integrated intensities at 77 and 300 K, which is associated with freezing-out of deep centers, decreased in this case. For example, before the diffusion of P this ratio was 17, while after the diffusion, it was only 3.3. Both these facts indicate that the concentration of the centers of nonradiative recombination decreases as a result of isovalent doping. The magnitude of the intensity ratio at various temperatures depended on the initial state of the surface of heteroepitaxial layers; however, it was always lower for the P-doped samples. This indicates that the diffusion of P leads to a considerable decrease in the surface recombination rate.

A small broadening of the PL band at $T = 300$ K from 46 to 53 meV after diffusion of P may be associated with an increase in the population in the valence band caused by an increase in the average lifetime of nonequilibrium carriers since, in the P-doped samples, broadening is accompanied by the shift of the peak to higher energies and by an increase in the total intensity.

To control the concentration of free carriers before and after the diffusion of P, the Raman spectra were measured. The Raman spectra have the shape characteristic of the lattice-matched InGaAs/InP alloys [9].

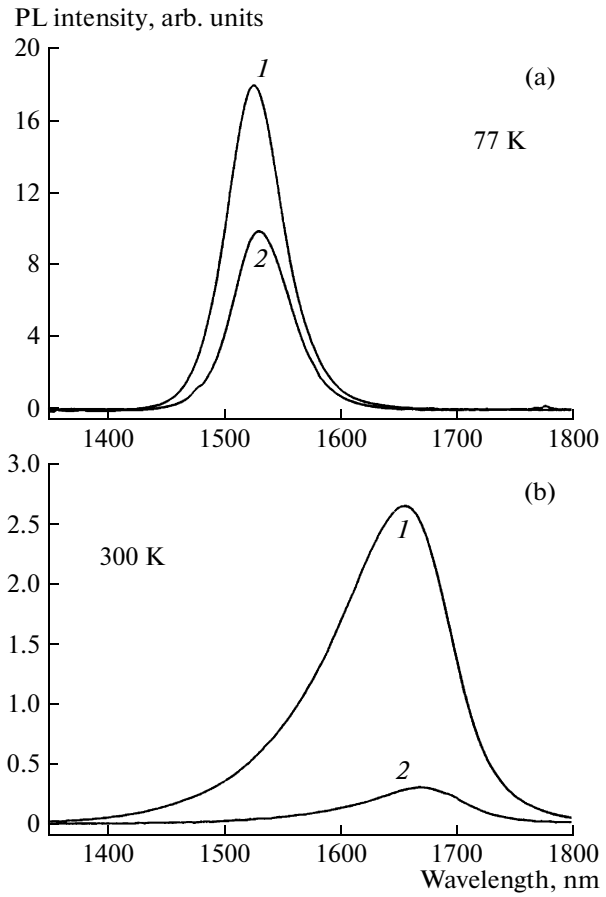

Fig. 2. Photoluminescence spectra of the InGaAs layers at (a) 77 and (b) 300 K: (*1*) the P-doped InGaAs layer and (*2*) undoped layer.

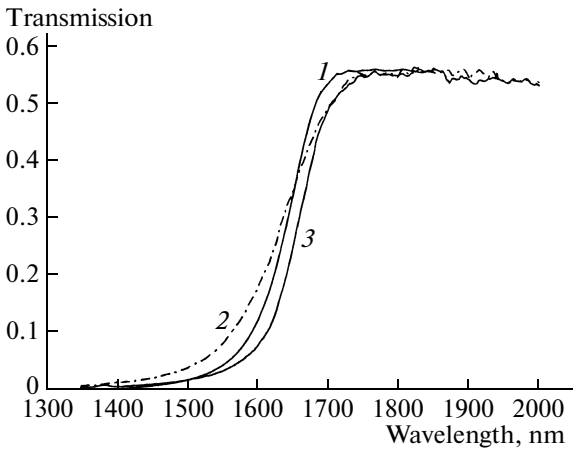

Fig. 3. Transmission spectra of the studied InP/InGaAs structures: (*1*) the as-grown InP/InGaAs *n*–*n* structure, (*2*) the structure with the *p*-type layer obtained without additional doping with P, and (*3*) the structure with the *p*-type layer and additional isovalent doping with P.

According to our measurements, the concentration of free carriers in studied layers was $(2–4) \times 10^{17}$ cm^{-3}. The analysis of the Raman spectra of the as-grown and isovalent-doped samples showed that the formation of the additional phase—specifically, the clusters of the InGaAs(P) alloy—does not occur in our experimental conditions. The comparison of the Raman spectra before and after the diffusion of P reveals their almost complete identity. This also indicates that the concentration of free electrons in reference and lattice-matched samples remains unchanged, i.e., the diffusion of P causes no increase in the carrier concentration, in contrast with the results of [10]. We can assume that, in our experimental conditions, the P atoms are incorporated into the anion sublattice of the alloy partially replacing the As atoms and decreasing the number of point defects without formation of additional donors.

3.2. p-InGaAs layers

Diffusion of Zn, similarly to that of any other impurity, is in many respects determined by defects existing in the material. In order to evaluate the effect of isovalent doping on the properties of Zn-doped InGaAs, we considered the transmission spectra of the as-grown *n*–*n* structure (Fig. 3, curve *1*) and structures, in which the *p*-alloy region (in our case, the base region of the photoconverter) was formed by the joint diffusion of Zn and P into the layer without additional isovalent doping with P (Fig. 3, curve *2*) and with it (Fig. 3, curve *3*). The as-grown *n*-InP structure/(*n*-InP buffer layer)/(*n*-InGaAs layer) was cleaved into three parts. One part remained as a reference sample (*n*–*n* structure), and diffusion of Zn was carried out into two other parts in corresponding modes that provided identical thickness of *p*-layers and impurity concentration on the surface of the InGaAs layer. From the results of the measurement of the Raman spectra, the concentration of electrically active impurity in the near-surface layer was $(1–2) \times 10^{19}$ cm^{-3}. We performed secondary ion mass spectroscopy (SIMS) measurements of the diffusion profile of Zn and concentration of P and H, which revealed a decrease in the concentration of H atoms in the structure with the additional diffusion of P.

The transmission spectra of the reference and *p*–*n* structures were measured at 300 K. The absorption edge of the structure with the additional diffusion of P (curve *3*) has a more abrupt slope compared with the structure without additional diffusion of P (curve *2*). At this stage of the study, it is difficult to determine what mechanism of interaction between the atoms of Zn, H, and P and occurring defects is responsible for the distinctions in the transmission spectra of the studied structures. However, we can definitely affirm that additional annealing in the vapors of P leads to a more uniform distribution of the Zn atoms over the bulk of the base region, which manifests itself in a more abrupt slope of the curve of the transmission spectrum.

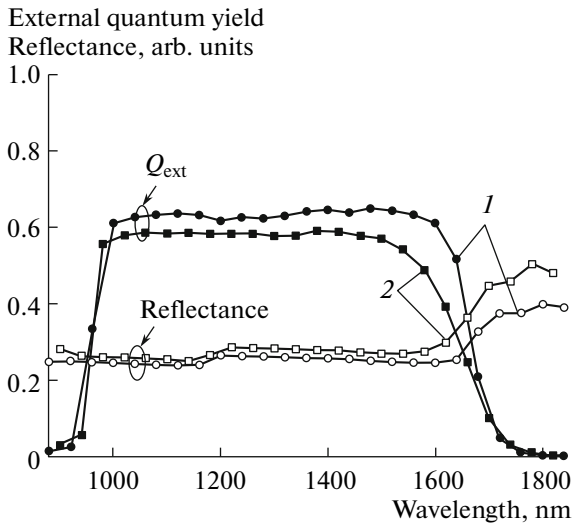

Fig. 4. External quantum efficiency (Q_{ext}) and reflectance spectra for the solar cells, transmission spectra of which are shown in Fig. 3: (*1*) the structure with additional isovalent doping and (*2*) the structure without additional isovalent doping. All structures are studied without antireflection coating.

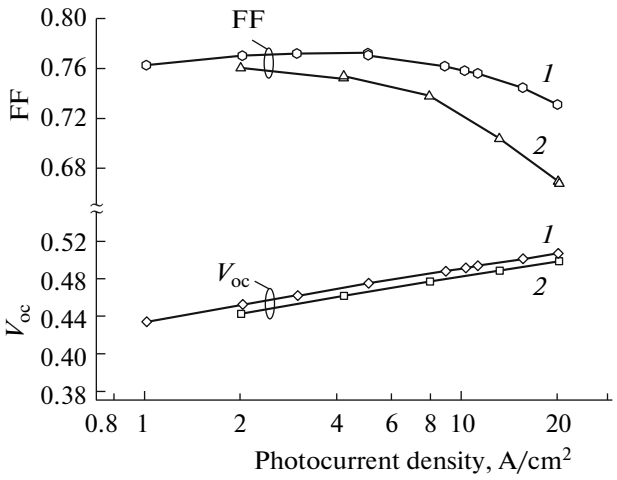

Fig. 5. Fill factor of the current–voltage characteristics and open-circuit voltage in to the photocurrent density for the InGaAs photocells with (curves *1*) and without (curves *2*) additional isovalent doping with P.

We also observed an increase in intensity of photoluminescence for the *p*-InGaAs layers with additional doping with P compared with the PL intensity of the layers without preliminary isovalent doping. It should be noted that the ratio of integrated PL intensities at 77 and 300 K for heavily Zn-doped *p*-InGaAs layers with $p = (3–5) \times 10^{19}$ cm^{-3} with additional isovalent doping is in the range of 2–4. Studies of PL intensity depending on temperature performed for lightly Zn-doped InGaAs layers ($p \approx 10^{16}$ cm^{-3}) obtained by the MOCVD method give the ratio of PL intensities at $T = 77$ and 300 K of 8–10 [11]. Therefore, the additional isovalent doping provides a considerable decrease in the contribution of nonradiative recombination even at a high level of Zn-doping of the layers, i.e., to decrease the number of defects both in the bulk and on the surface of the *p*-layer.

4. CHARACTERISTICS OF InGaAs PHOTOCONVERTERS

4.1. Quantum Efficiency

The external quantum efficiency of photocells fabricated based on the heterostructures the transmission spectra of which are shown in Fig. 3 is presented in Fig. 4. As noted above, the thicknesses of the *n*- and *p*-type regions of the structures and the doping levels are identical; consequently, we can assume that the improvement of the spectral characteristic of the cell with the additional isovalent doping is associated with lowering the concentration of defects in the alloy bulk. It is noteworthy that the largest difference in the spectra is observed in the long-wavelength region, which indicates an increase in the diffusion length of minority carriers in the *p*-type layer, which is possibly caused by the more uniform distribution of the Zn atoms.

4.2. Fill Factor of the Current–Voltage Characteristic and the Open-Circuit Voltage

It is known that the main parameter affecting the magnitude of the fill factor (FF) is the reverse saturation current (dark current), a decrease in which leads to an increase in the FF [12]. The measurement and comparison of dark resistanceless current–voltage characteristics of solar cells were performed by the procedure of [13]. The smallest diffusion preexponential multiplier J_{0d} and, consequently, the longest lifetime of nonequilibrium carriers $\tau_{pN} \approx 10^{-9}$ s in a quasineutral *n*-type region were observed for the structure with additional isovalent doping. The mentioned parameters are approximately an order of magnitude larger than for the sample without additional doping with P.

Figure 5 shows the variations in the FF and V_{oc} in relation to the current density for the samples, the quantum efficiency of which is presented in Fig. 3. The concentrations of majority carriers in the *n*- and *p*-type regions of these cells are identical. As evident from Fig. 5, the values of FF and V_{oc} for solar cells with additional doping are larger over the entire range of the values of the current density. An increase in the fill factor of the *I–V* characteristic for the photocells with additional isovalent doping is also caused by considerably lower ohmic losses. In this case, the Cr/Au low-resistance contact to the base region of the photocell is formed on a heavily doped *p*-InGaAs layer with a decreased amount of defects, which was mentioned above.

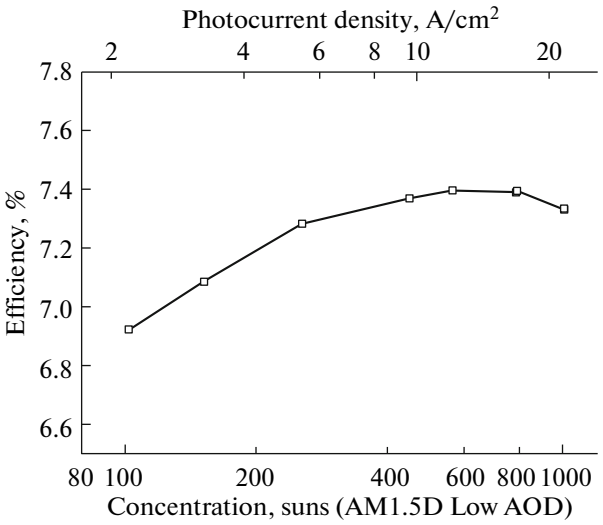

Fig. 6. Conversion efficiency of the InP/InGaAs-based inverted solar cell with additional isovalent doping. The spectrum of solar radiation was AM1.5D Low AOD.

4.3. Conversion Efficiency of the Solar Cell

Figure 6 shows the efficiency of the InGaAs solar cell with additional isovalent doping. For this type of cell, the range of photosensitivity is in the limits of 880–1840 nm due to complete absorption of the short-wavelength radiation by the InP substrate. The photocurrent density is 19.3 mA/cm^2 in recalculation to the active surface irradiated by the solar radiation with the AM1.5 Low AOD spectrum (1000 W/m^2). The thickness of the emitter region was 2 μm. At this stage of the studies, no optimization of the thickness of the emitter region of the photocell and, consequently, photocurrent density was carried out. The maximum spectral efficiency of the photovoltaic converter in a spectral range of 900–1840 nm remained at a level of 7.4–7.35% with a ratio of concentration of solar radiation of 500–1000.

The developed InGaAs photoconverters can be successfully used as a narrow-gap cascade in mechanically joined tandem solar cells with an upper wide-gap stage based on the InGaP–GaAs system [14] providing total efficiency higher than 35%.

5. CONCLUSIONS

As a result of the studies, it is established that the additional isovalent doping with P of the InGaAs alloys substantially improves the surface and bulk properties of the layers. The base technology developed with the use of liquid-phase epitaxy and single-stage diffusion of isovalent and doping impurities allows one to develop highly efficient narrow-gap solar cells for conversion of concentrated solar radiation in a range of 100–1000 suns. This technology can be successfully used for other III–V materials.

ACKNOWLEDGMENTS

We thank V.D. Rumyantsev for helpful discussions, V.S. Kalinovskii for measurements of dark characteristics of the InGaAs photoconverters, and B.Ya. Ber and A.P. Kovarskii for measurements of concentration profiles of the doping and isovalent impurities by secondary ion mass spectroscopy.

REFERENCES

1. D. M. Wilt, R. Wehrer, M. Palmisiano, M. Wanlass, and Ch. Murray, Semicond. Sci. Technol. **18**, S209 (2003).
2. M. Emziane and R. J. Nicholas, Appl. Phys. **101**, 054503 (2007).
3. L. B. Karlina, B. J. Ber, M. M. Kalugina, A. P. Kovarsky, C. Vargas-Aburto, R. M. Uribe, D. Brinker, and D. Scheiman, in *Proc. of the 28th IEEE PVSC* (Alaska, 2000), p. 1230.
4. L. B. Karlina, M. M. Kulagina, M. Z. Shvarts, A. S. Vlasov, and V. M. Andreev, in *Proc. of the 21st Eur. Photovoltaic Solar Energy Conf.* (Dresden, 2006), p. 473.
5. L. B. Karlina, A. S. Vlasov, M. M. Kulagina, and N. Kh. Timoshina, Fiz. Tekh. Poluprovodn. **40**, 351 (2006) [Semiconductors **40**, 346 (2006)].
6. A. Jalil, B. Theys, J. Chevallier, A. M. Huder, C. Grattepain, and P. Hietz, Appl. Phys. Lett. **57**, 2791 (1990).
7. B. Karlina, M. M. Kulagina, N. Kh. Timoshina, A. S. Vlasov, and V. M. Andreev, in *Proc. of the 7th World TPV Conf. Thermophotovoltaic Generation of Electricity* (Madrid, Spain, 2006), p. 182.
8. M. A. Steiner, J. F. Geisz, R. C. Reedy, Jr., and S. Kurtz, in *Proc. of the 33rd IEEE Photovoltaic Specialists Conf.* (San Diego, 2008), p. 143.
9. A. M. Mintairov and H. Temkin, Phys. Rev. B **55**, 5117 (1997).
10. S. Hernandez, N. Blanko, I. Martil, G. Gonzalez-Diaz, R. Cusco, and L. Artus, J. Appl. Phys. **93**, 9019 (2003).
11. D. Donetsky, S. Anikeev, N. Gu, M. Dashiell, H. Ehsani, F. Newman, M. Wanlass, and C. Wang, in *Proc. of the 4th World Conf. on Photovoltaic Energy Conversion* (Hawaii, 2006), p. 764.
12. V. M. Andreev, V. A. Grilikhes, and V. D. Rumyantsev, *Photoelectric Converters of Concentrated Solar Radiation* (Nauka, Leningrad, 1989) [in Russian].
13. L. B. Karlina, V. V. Evstropov, V. S. Kalinovsky, M. M. Kulagina, N. H. Timoshina, A. V. Vlasov, and V. M. Andreev, in *Proc. of the 22 Eur. Photovoltaic Solar Energy Conf.* (Milan, 2007), p. 520.
14. P. R. Sharps, A. Cornfeld, M. Stan, and A. Korostyshevsky, in *Proc. of the 33rd IEEE Photovoltaic Specialists Conf.* (San Diego, 2008), p. 511.

Translated by N. Korovin